Supplementary information

The Langmuir-Schaeffer technique as a method for controlled alignment of 1D materials

Michal Bodik[a*], Ondrej Maxian[b], Jakub Hagara[a], Peter Nadazdy[a], Matej Jergel[a], Eva Majkova[a,c] and Peter Siffalovic[a,c]

[a] Institute of Physics, Slovak Academy of Sciences, Dubravska cesta 9, 845 11 Bratislava, Slovakia

[b] Courant Institute of Mathematical Sciences, New York University. 251 Mercer St., New York, New York 10003, United States of America

[c] Centre for Advanced Materials Application, Dubravska cesta 9, 845 11 Bratislava, Slovakia

*corresponding author, email: Michal.Bodik@savba.sk

Contents

Langmuir-Schaeffer deposition

The repeatability of the SWCNT Langmuir film formation was checked by performing several experimental runs (Fig. S1). The amount of material dropped onto the subphase was changed in between the different film compressions in order to check the behavior of the SWCNT films at higher surface pressures. The form of the pressure-area (Π-A) isotherm is well reproduced; only the starting conditions are different. The offset of the measured isotherms is caused by the different amounts of material dropped before the compression.

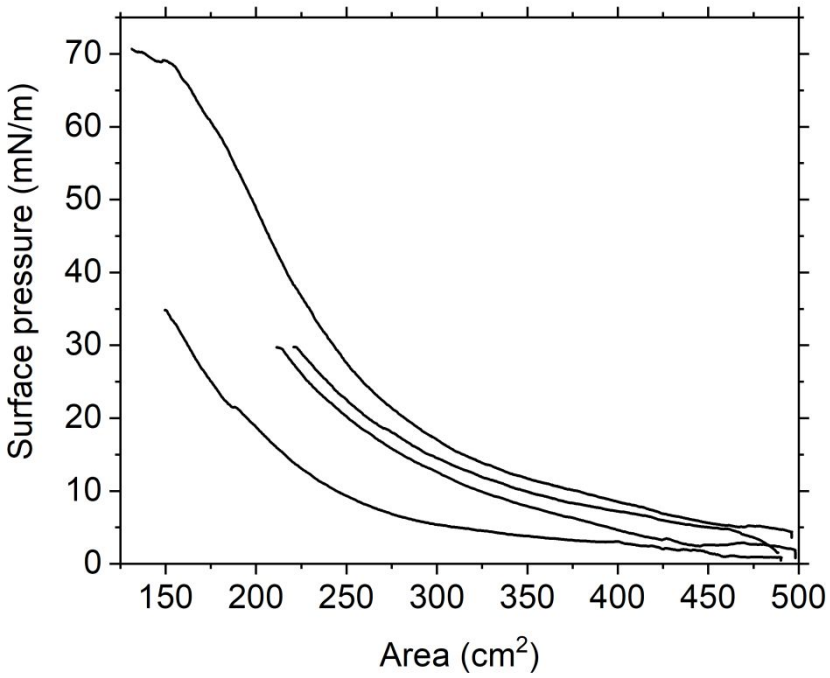

Fig. S1: The surface Π-A isotherms for different amounts of material dropped onto the subphase.

***In-situ* Raman microspectroscopy**

To further study the orientation during the formation of SWCNTs Langmuir films, we performed several experiments with polarized Raman microspectroscopy. Fig. S2 shows the experimental setup of in-situ confocal Raman microspectroscopy on the water subphase. We changed the closing speed of barriers to support the simulation results that the alignment will be observable for flow speeds on the order 10 cm/min. Fig. S3 – S7 show the evolution of the Π-A isotherms and orientation parameter during the *in-situ* Raman measurements with different closing speeds.

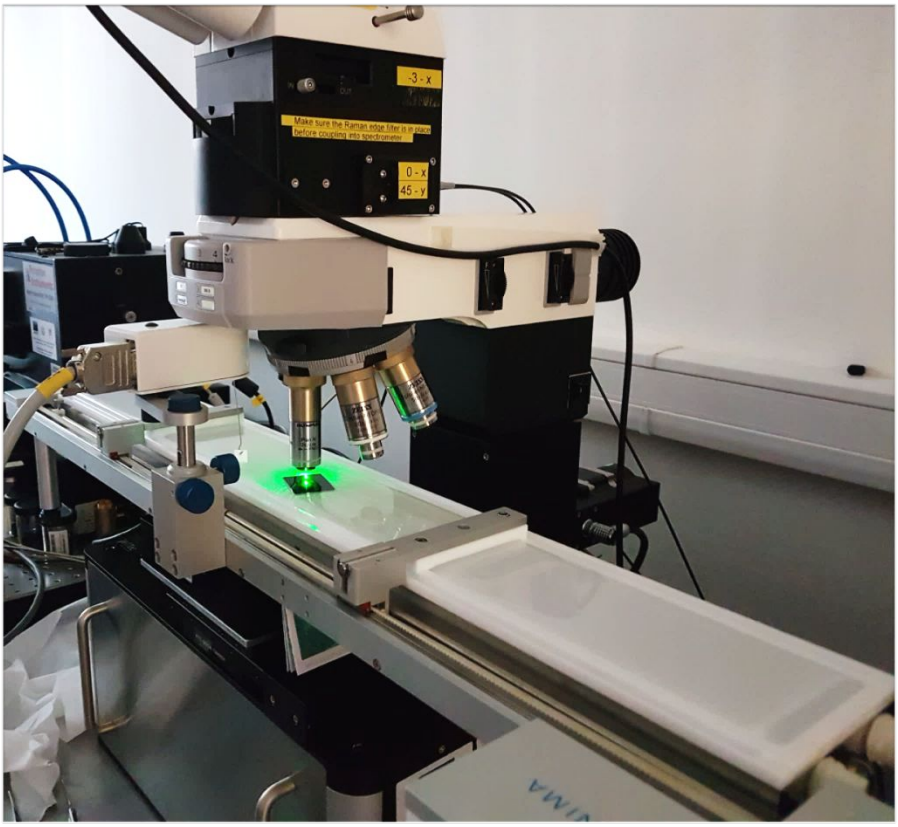

Fig. S2: A photograph of the in-situ confocal Raman microspectroscopy experimental set-up.

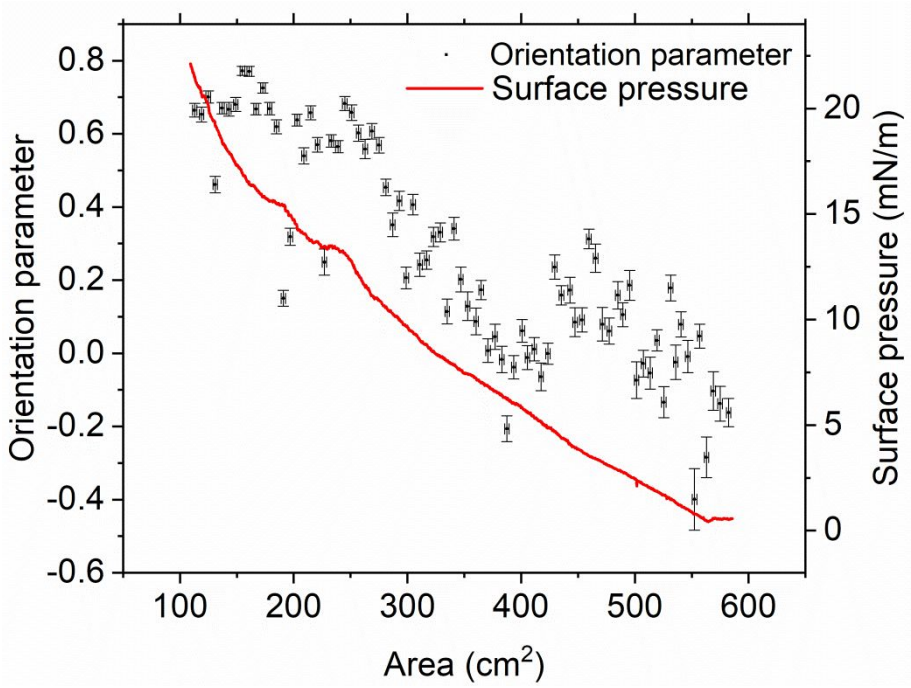

Fig. S3: The evolution of the Π-A isotherm (red line) and orientation parameter (black dots) during the compression with a barrier speed of 5 mm/min.

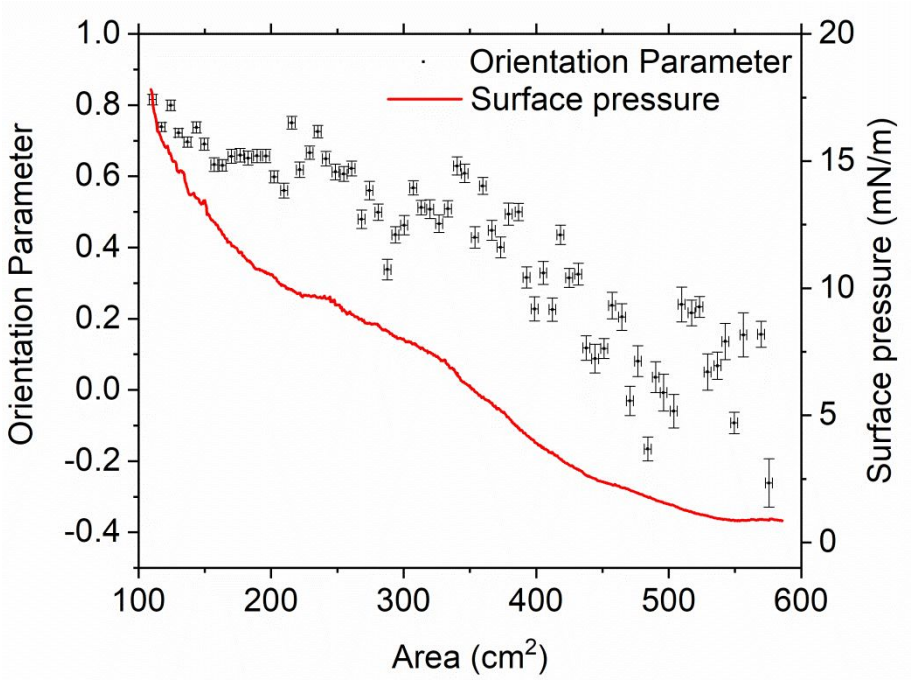

Fig. S4: The evolution of the Π-A isotherm (red line) and orientation parameter (black dots) during the compression with a barrier speed of 10 mm/min.

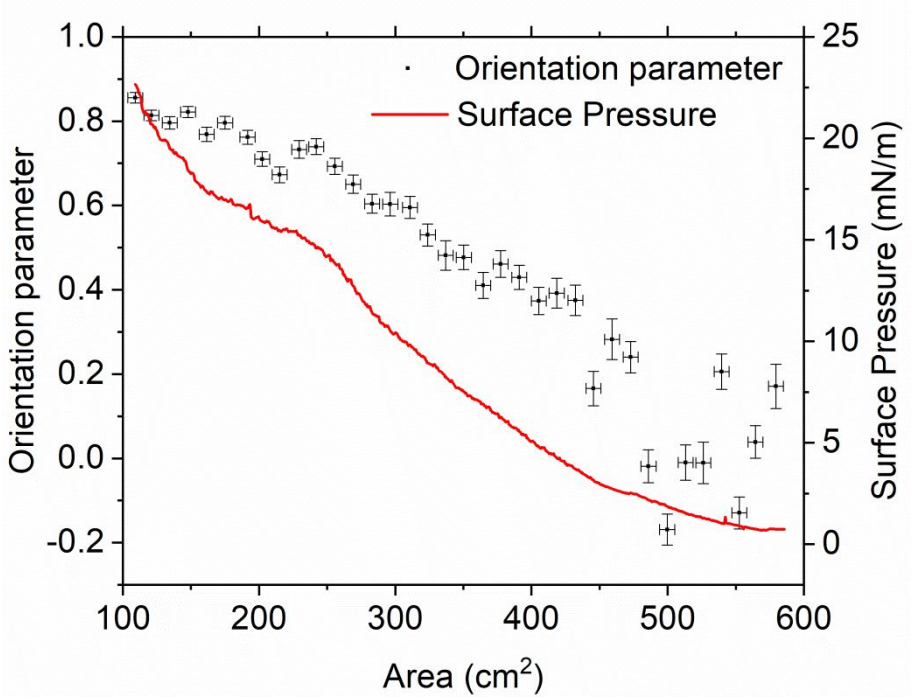

Fig. S5: The evolution of the Π-A isotherm (red line) and orientation parameter (black dots) during the compression with a barrier speed of 20 mm/min.

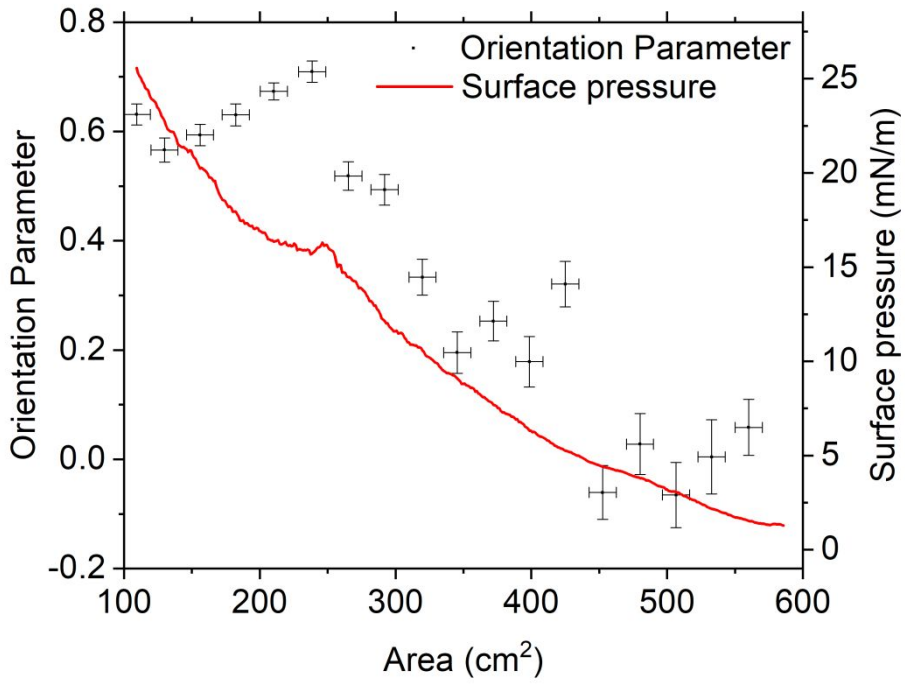

Fig. S6: The evolution of the Π-A isotherm (red line) and orientation parameter (black dots) during the compression with a barrier speed of 40 mm/min.

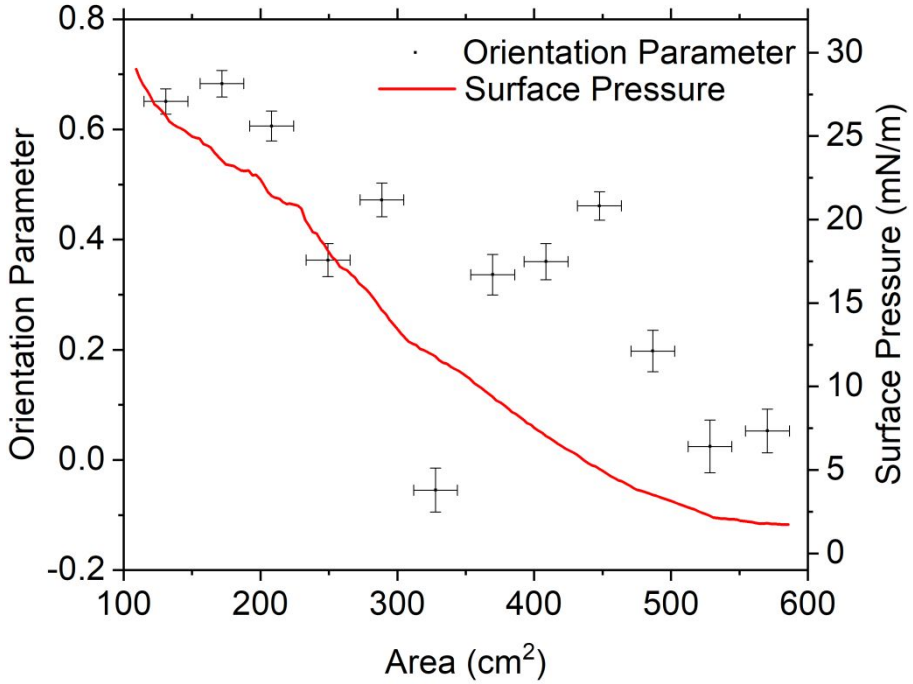

Fig. S7: The evolution of the Π-A isotherm (red line) and orientation parameter (black dots) during the compression with a barrier speed of 100 mm/min.

Because of the different starting conditions, we compared different measurements of the orientation parameter also as a function of surface pressure, rather than the Langmuir film area. The surface pressure (Π) is more reliable as it depends on the coverage of the SWCNTs on the water subphase. We plotted the experimentally obtained data of orientation parameter from Fig. S3 – S7 as a function of surface pressure in Fig. S8 – S11. Except for one experiment with a barrier speed of 10 mm/min, the evolution of the orientation parameter follows the same trend. From the random starting orientation, in the course of compression the SWCNTs gradually orient and reach an orientation parameter around 0.8 at a surface pressure close to 20 mN/m.

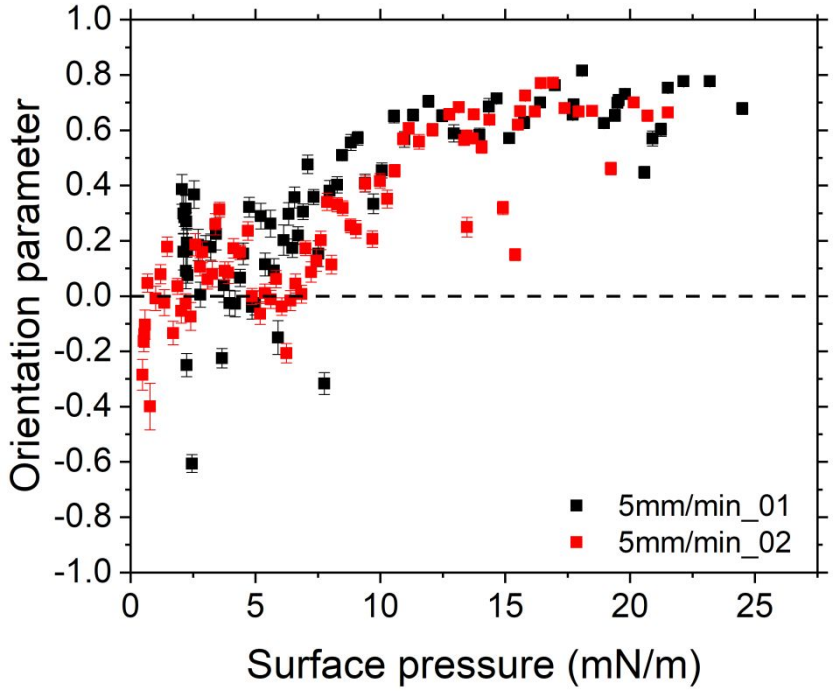

Fig. S8: The evolution of the orientation parameter as a function of the surface pressure for measurements obtained with a closing speed of 5 mm/min.

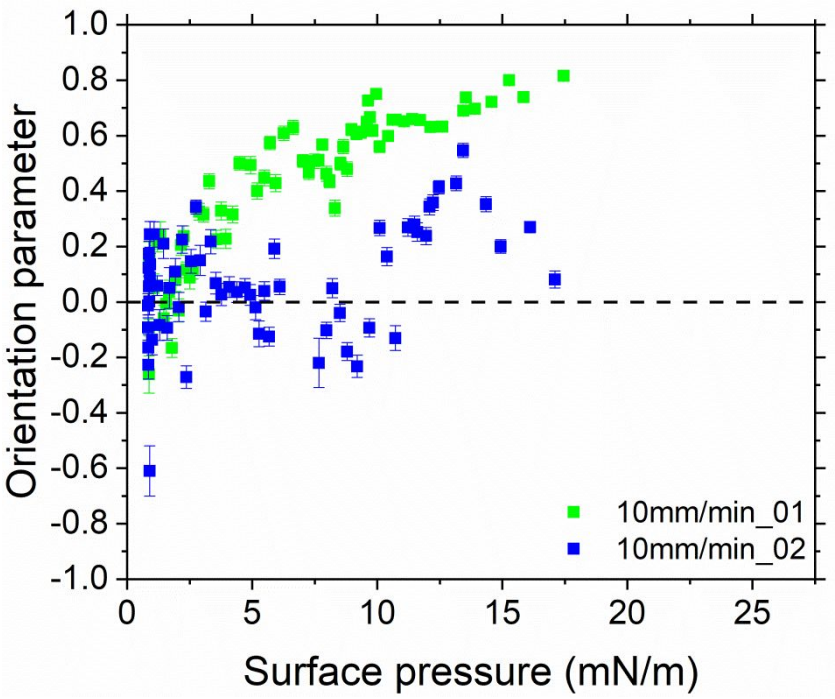

Fig. S9: The evolution of the orientation parameter as a function of the surface pressure for measurements obtained with the closing speed of 10 mm/min.

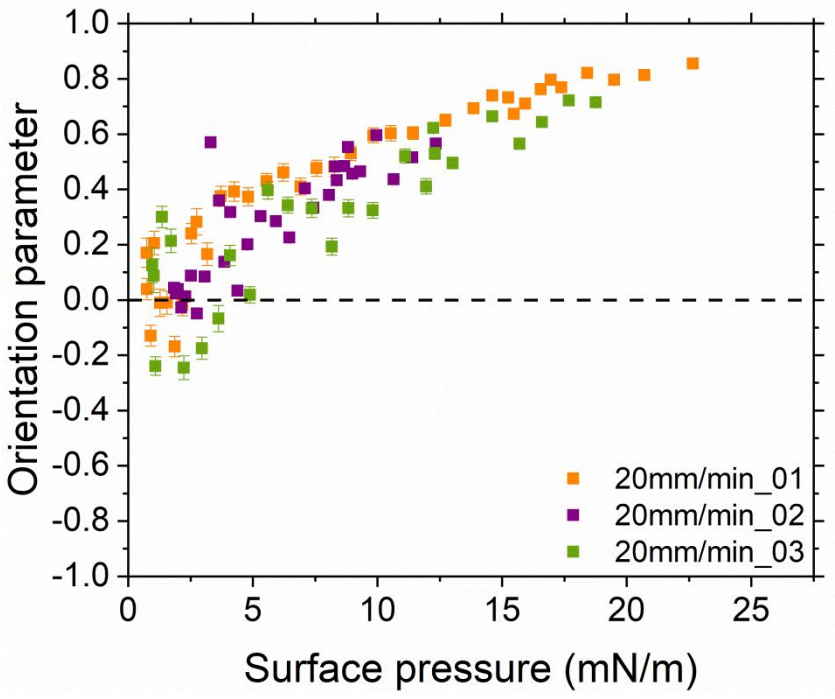

Fig. S10: The evolution of the orientation parameter as a function of the surface pressure for measurements obtained with the closing speed of 20 mm/min.

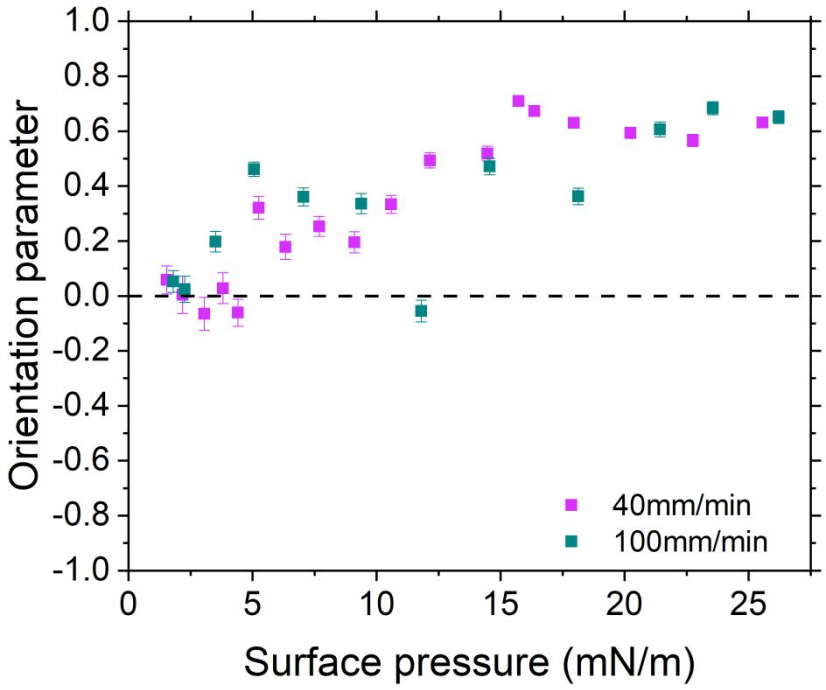

Fig. S11: The evolution of the orientation parameter as a function of the surface pressure for measurements obtained with closing speeds of 40 mm/min and 100 mm/min.

Evaluation of the mechanical stress during the Langmuir film compression

The compression of the Langmuir film can induce mechanical stress of CNTs. The position of Raman bands depends on the mechanical stress applied to the CNTs [1]–[4]. Fig. S12 shows the evolution of the position of both G and 2D bands as a function of the surface pressure. We observed only shifts with a magnitude less than 1 cm^{-1} in the position of both bands, which is below the instrumental resolution of our Raman spectrophotometer. These results suggest that the stress induced by the moving barriers on the CNTs is negligible.

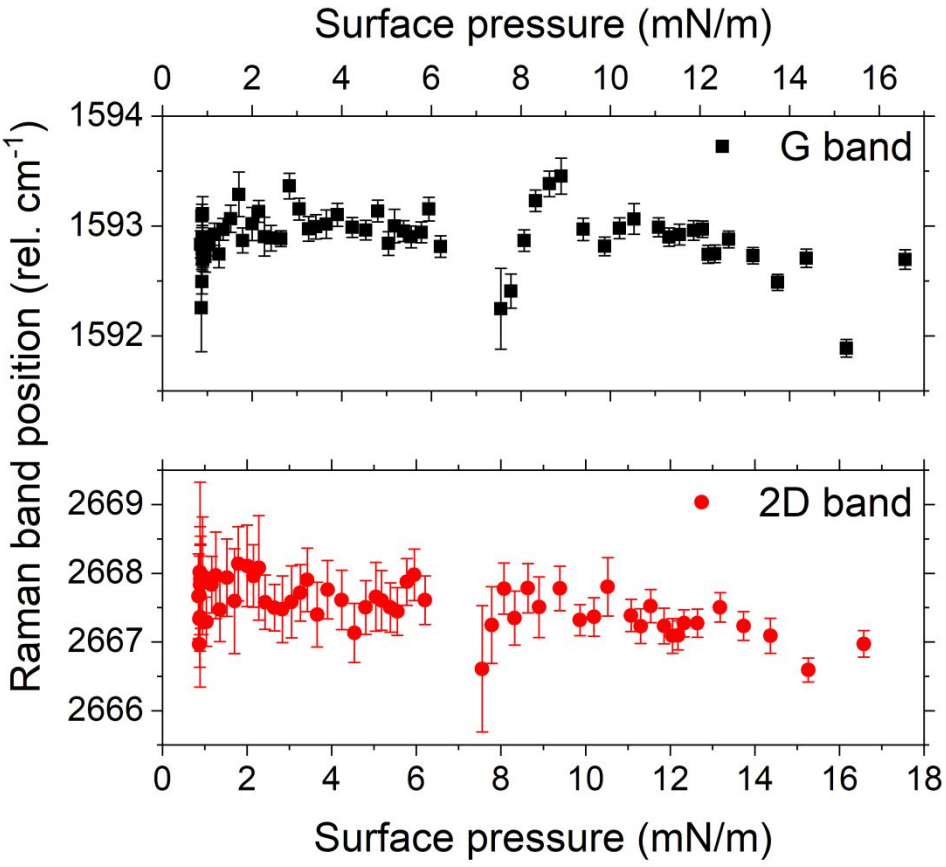

Fig. S12: The position of the Raman G-band (top) and 2D-band (bottom) during the compression of the CNT film.

***Ex-situ* Grazing-incidence small-angle X-ray scattering (GISAXS)**

Furthermore, we confirmed the SWCNTs alignment on a macroscopic scale using grazing-incidence small-angle X-ray scattering (GISAXS). While the Raman microspectroscopy and AFM are local methods and the probing area is limited to approximately 100 μm^2, using GISAXS we can collect information across the whole substrate surface. This gives us statistically relevant information on SWCNT alignment over a large area and confirms that the alignment is not only local.

The GISAXS experiments were measured on a custom-designed Nanostar system (Bruker AXS, Germany) equipped with a liquid-metal jet X-ray source (MetalJet D2, Excillum). The X-ray emission with a wavelength of 0.134 nm (Ga Kα) was collected using a

reflective Montel optics and further collimated by a set of two 300 μm pinholes separated by a distance of 500 mm. The angle of incidence was set to 0.2°. The scattered X-ray radiation was detected by a two-dimensional X-ray detector (Pilatus 300K, Dectris).

We performed two mutually orthogonal GISAXS measurements after the transfer of the Langmuir film to a silicon substrate. In one case, the oriented SWCNTs were aligned along the beam direction and in the second case the SWCNTs were aligned perpendicular to the impinging X-ray beam. The X-ray scattering profiles measured in these two configurations are shown in Fig. S13.

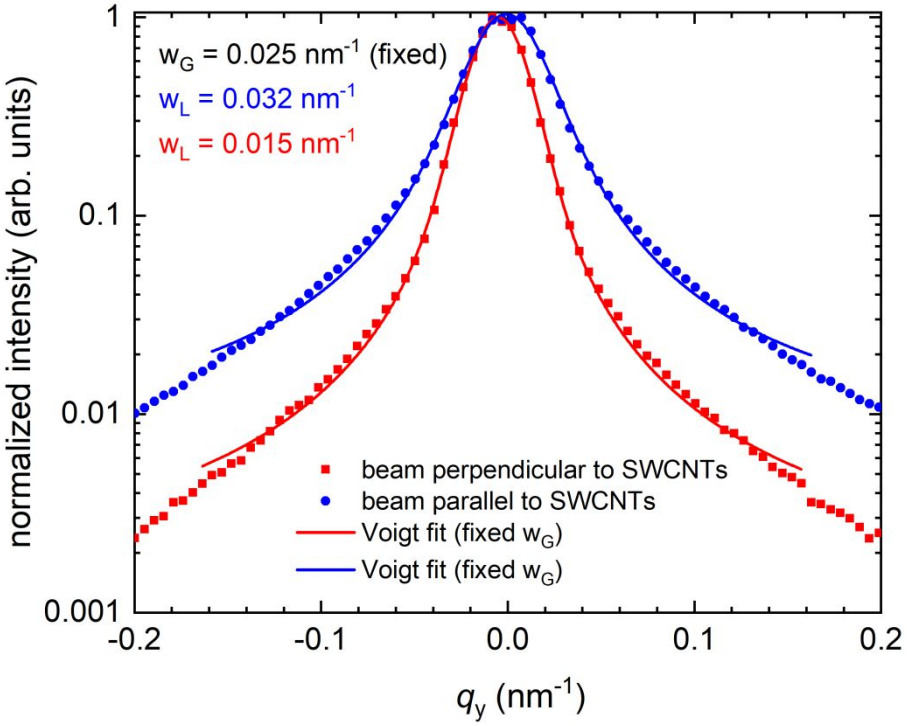

Fig. S13: The GISAXS pattern for the film of SWCNTs aligned parallel (blue circles) and perpendicular (red squares) to the impinging X-ray beam.

The intensity profiles were integrated between the in-plane exit angles starting from 0.3° to 0.45°. The intensity profiles can be successfully fitted by the Voigt peak function, i.e. a convolution of Gaussian and Lorentz peak functions. Both fits share an identical Gaussian function, which describes the instrumental resolution of the experimental setup. In the first approximation, the Lorentz functions are used to describe the broadening due to the aligned

Langmuir film of SWCNTs. It is obvious that the width of scattering curve (blue) recorded in the geometry when the X-ray beam is parallel with the aligned SWCNTs is doubled when compared to the width of the scattering curve recorded in the perpendicular geometry. In general, the GISAXS pattern is given as a product of a form-factor and interference function[5]. The observed broadening is an interplay of the oriented form factor function of SWCNTs and their interference function. A limited short-range order in the ensemble of aligned SWCNTs prevented observation of distinct maxima in the scattering pattern characteristic of long-range ordered nanomaterials[6]. Nevertheless, a pronounced broadening of the scattering curve measured in the parallel geometry supports a global alignment of SWCNTs probed locally by in-situ Raman and ex-situ AFM measurements.

Results for the numerical simulations

This section has two parts: first, we show a typical simulation, where the initial trough half-width $w_0 = 12.5$ cm. Next, we analyze the contributions of the parameters ϵ and v_w to the alignment of the SWCNTs and show what parameter sets give the best alignment.

Typical simulation

Fig. S14 shows snapshots of a system of 20 SWCNTs with length 2 μm being compressed with $v_w = 10$ cm/min. For this simulation, we set $\epsilon = 20$ nm, since the tube agglomerates in our experiments were observed to have an equilibrium spacing that is approximately 20-30 nm. We observe qualitatively that the tubes initially draw closer together due to the attractive forces, and then towards the end of the simulation are aligned in the y direction by the fluid motion.

Fig. S15 shows the values of the orientation parameter $\phi(t)$ for the same simulation shown in Fig. S14. The quantitative study confirms what was observed in Fig. S14; the

alignment of the CNTs really happens in the second phase of the compression in the Langmuir trough. In other words, the more tightly packed the CNTs are, the greater the effect of compressing the trough. This agrees with experimental results that showed a higher degree of alignment for high surface pressures (tighter packing).

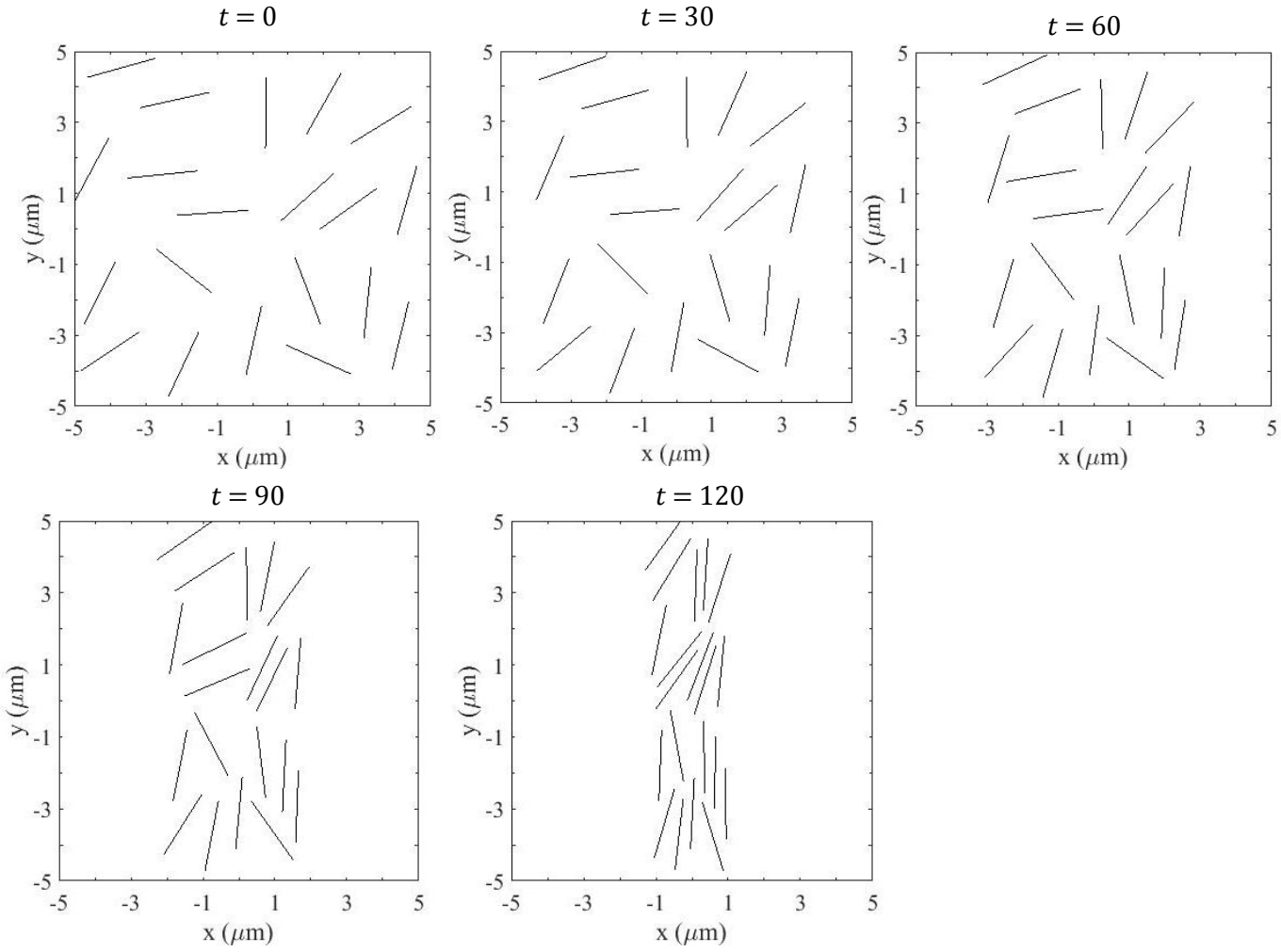

Figure S14: Snapshots of 20 carbon nanotubes being compressed on a 10 μm $\times$ 10 μm square at the center of the Langmuir trough with $w_0 = 12.5$ cm, $\epsilon =$ 20 nm, $v_w = 10$ cm/min. Pictures are shown at 5 time points (in seconds) that correspond to 0, 20, 40, 60, and 80% compression (80% being the trough limit). It is clear that the alignment takes place primarily between the last two frames (between 60 and 80% compression).

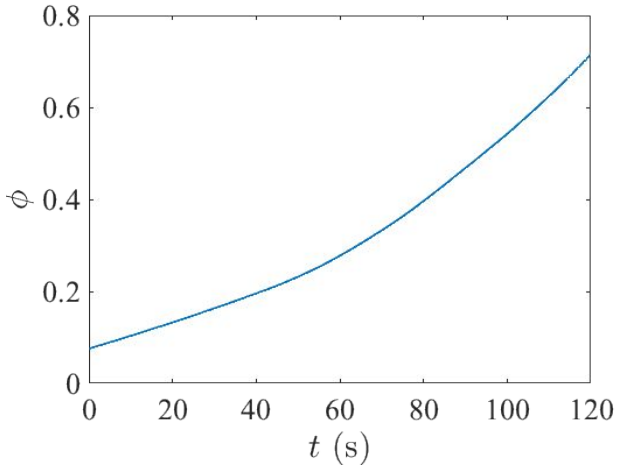

Figure S15: Orientation parameter ϕ over time for the system shown in Figure S15. The CNTs tend to align when they are packed more tightly together (later in the simulation). This confirms experimental findings that show a higher degree of alignment with higher surface pressure.

Changing the parameter balance

When attractive forces dominate the flow speed, the degree of alignment is reduced. As shown in Fig. S16, where ϵ has decreased to 10 nm and v_w has also decreased to 1 cm/min, this trend occurs because of the tendency of CNTs to become locked together in bundles when the velocity induced by the attractive forces is stronger than the fluid flow. These bundles do not break apart in time because the force (shear gradient) of the fluid is insufficient to overcome the required increase in potential energy. As shown in Fig. S17, this results in the alignment parameter ϕ oscillating through time as the CNTs seek to minimize their potential energy, regardless of the direction of alignment.

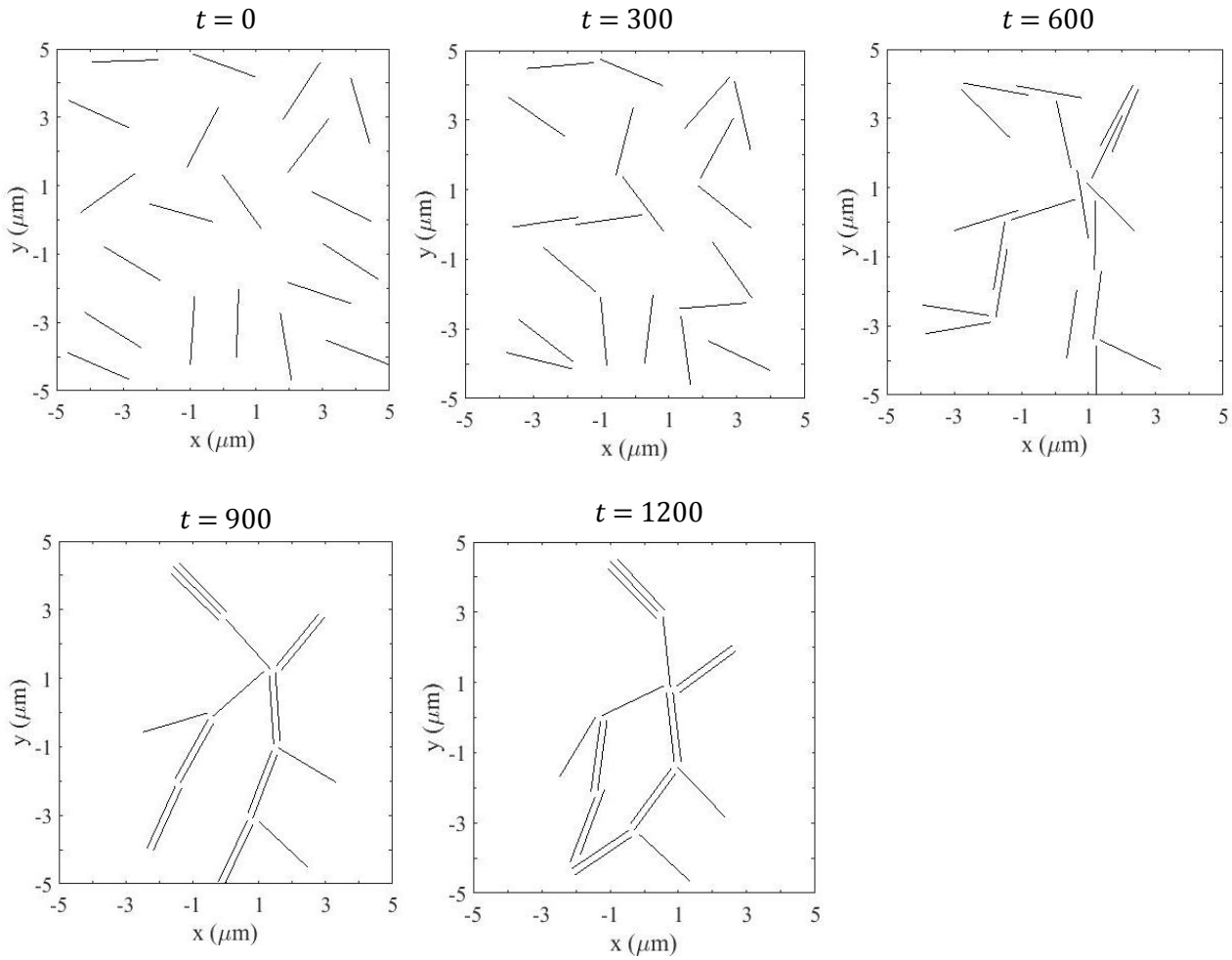

Figure S16: Snapshots of 20 carbon nanotubes being compressed on a 10 μm $\times$ 10 μm square at the center of the Langmuir trough with $w_0 = 12.5$ cm, $\epsilon =$ 10 nm and $v_w = 1$ cm/min. Notice that ϵ and v_w have both decreased from Fig. S13, indicating a stronger attractive force and weaker shear gradient. As before, the time values (in seconds) correspond to 0, 20, 40, 60, and 80% compression. CNTs with a large attractive force between them form bundles that become locked together and cannot be oriented by the slow fluid motion.

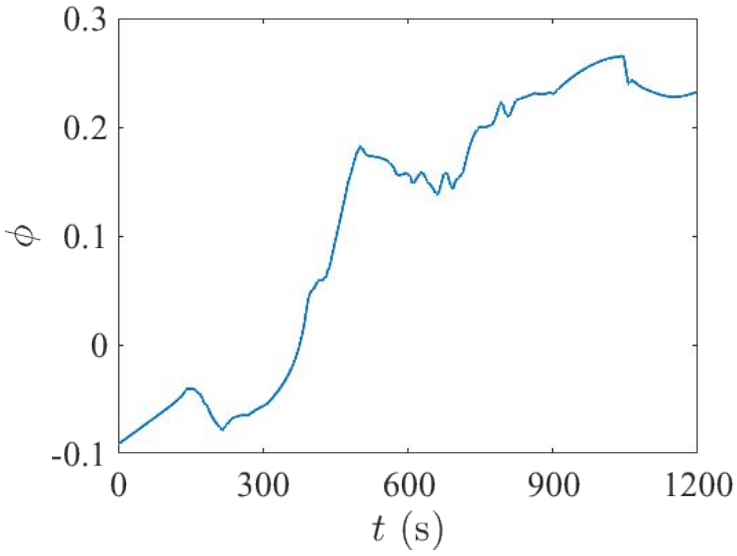

Figure S17: Orientation parameter over time for $\epsilon =$ 10 nm, $v_w = 1$ cm/min. There is initially some alignment, but the stronger attractive forces dominate once the CNTs are pushed close together (beyond 40% compression = 600 s). These attractions prevent the CNTs from properly aligning, which results in a randomly fluctuating alignment parameter at the end of the compression cycle.

Changing the interaction of CNTs

To test whether only the immediate interactions are important, we calculated the trajectory of the same 80 CNTs as in manuscript Fig. 4(b), but this time only considering neighboring CNTs (defined as those separated by a minimum distance of 20ϵ or less). This means that we are only including repulsive forces due to the potential. The CNTs are not attracting each other since velocities due to CNTs farther than 20ϵ are set to zero.

As shown in the Fig. S18, using only repulsive interactions gives approximately the same trajectory for the orientation parameter as using all interactions. The conclusion is therefore that alignment from the flow combined with steric repulsion is enough to align the CNTs. Long-range attraction is not a necessary component. This supports our main conclusions since the goal of the surfactant is to eliminate attractive forces.

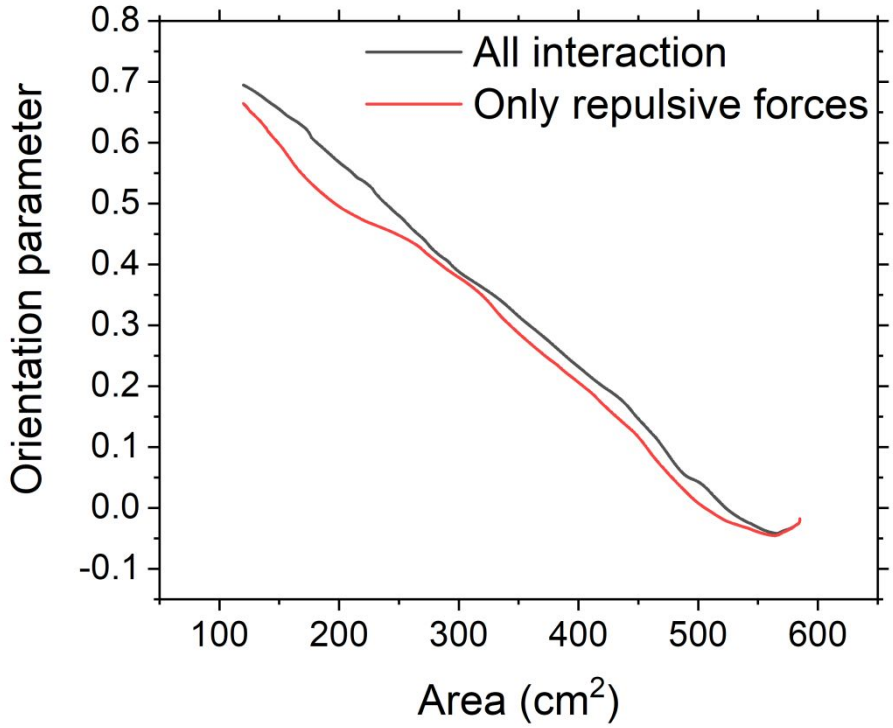

Figure S18: The evolution of the orientation parameter during compression for a simulation of 80 CNTs with $\epsilon = 30$ nm and $v_w = 2$ cm/min (same parameters as in Fig. 4(b) of the main text). We compare the case when only repulsive forces between CNTs are included (red line) to the case where CNTs attract each other at long range and repel at short range (black line). The similarity between the two curves suggests that long range attractive forces between CNTs play little role.

References

[1] Q. Zhao, M. D. Frogley, and H. D. Wagner, "Direction-sensitive strain-mapping with carbon nanotube sensors," *Compos. Sci. Technol.*, vol. 62, no. 1, pp. 147–150, Jan. 2002.

[2] Q. Zhao, M. D. Frogley, and H. D. Wagner, "The use of carbon nanotubes to sense matrix stresses around a single glass fiber," *Compos. Sci. Technol.*, vol. 61, no. 14, pp. 2139–2143, Nov. 2001.

[3] J. R. Wood, Q. Zhao, and H. D. Wagner, "Orientation of carbon nanotubes in polymers and its detection by Raman spectroscopy," *Compos. Part A Appl. Sci. Manuf.*, vol. 32, no. 3–4, pp. 391–399, Mar. 2001.

[4] M. Mu, S. Osswald, Y. Gogotsi, and K. I. Winey, “An in situ Raman spectroscopy study of stress transfer between carbon nanotubes and polymer,” *Nanotechnology*, vol. 20, no. 33, p. 335703, Aug. 2009.

[5] G. Renaud, R. Lazzari, and F. Leroy, “Probing surface and interface morphology with Grazing Incidence Small Angle X-Ray Scattering,” *Surf. Sci. Rep.*, vol. 64, no. 8, pp. 255–380, Aug. 2009.

[6] G. Renaud, R. Lazzari, and F. Leroy, “Probing surface and interface morphology with Grazing Incidence Small Angle X-Ray Scattering,” *Surf. Sci. Rep.*, vol. 64, no. 8, pp. 255–380, Aug. 2009.